# Beyond Universal Saliency: Personalized Saliency Prediction with Multi-task CNN

Anonymous

## Abstract

Saliency detection is a long standing problem in computer vision. Tremendous efforts have been focused on exploring a universal saliency model across users despite their differences in gender, race, age, *etc.* . Yet recent psychology studies suggest that saliency is highly specific than universal: individuals exhibit heterogeneous gaze patterns when viewing an identical scene containing multiple salient objects.

In this paper, we first show through an experiment that such heterogeneity is common and critical for reliable saliency prediction. Our study also produces the first database of personalized saliency maps (PSMs). We propose to model PSM based on universal saliency map (USM) shared by different participants and adopt a multi-task CNN framework to estimate the discrepancy between PSM and USM. Comprehensive experiments demonstrate that our new PSM model and prediction scheme are effective and reliable.

## 1 Introduction

Saliency refers to a component (object, pixel, person) in a scene that stands out relative to its neighbors and has been considered key to human perception and cognition. Traditional saliency detection techniques attempt to extract the most pertinent subset of the captured sensory data (RGB images or light fields) for predicting human visual attention. Applications are numerous, ranging from compression [Itti, 2004] to image re-targeting [Setlur *et al.*, 2005], and most recently to virtual reality and augmented reality [Chang *et al.*, 2016].

By far, nearly all previous approaches have focused on exploring a universal saliency model, i.e., to predict potential salient regions common to users while ignoring their differences in gender, race, age, personality, etc. Such universal solutions are beneficial in the sense they are able to capture all "potential" saliency regions. Yet they are insufficient in recognizing heterogeneity across individuals. Examples in Fig. 1 illustrate that while multiple objects are deemed highly salient within the same image (eg, *human face* (first row), *text* (last tow rows) and object of (*high color contrast*), different individuals have very different fixation preferences when viewing the image. For the rest of the paper, we use term *universal saliency* to describe salient regions that incur high fixations across all subjects and term *personalized saliency* to describe the heterogeneous ones.

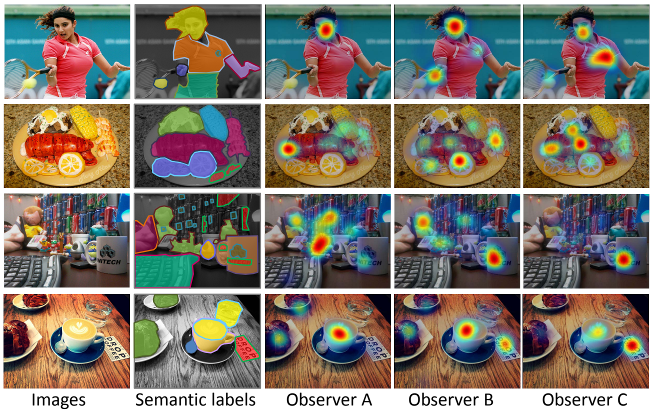

Figure 1: An illustration of PSM dataset. Our dataset provides both eye fixations of different subjects and semantic labels. Due to the large amount of objects in our dataset, for each image, we didn't full segment it and only labelled objects covering at least three gaze points of each individual. A notable difference between PSM and its predecessors is that each subjects looks 4 times on PSM data to derive solid fixation ground truth maps. Both commonality and distinctiveness exist for PSMs viewed by different participant. This motivates us to model PSM based on USM.

**Motivation.** In fact, heterogeneity in saliency preference has been widely recognized in psychology: "Interestingness is highly subjective and there are individuals who did not consider any image interesting in some sequences" [Gygli *et al.*, 2013]. Therefore, once we know someone's personalized interestingness over each image (personalized saliency), some algorithms can be designed which can better cater him/her needs. Say in image retargeting application, for the image in the fourth row in Fig. 1, the text on the table should be preserved for observer B and C when resizing the image, while it is not necessary to be kept for observer A. For some applications in VR/AR setting, for example, we can design data compression algorithms that personalized salient regions should be less compressed in order to both improve the users' experience and reduce the size of data in transmission; We can embed some characters/logo/advertisement at those personalized salient regions for different persons. There are also some other potential personalized saliency detection applications which won't be discussed because of the paper length constraint. However, in computer vision, very little work has been carried out on studying such heterogeneity, partially due to the lack of suitable dataset and experiments. Further, the problem is also inherently challenging as saliency variations across individual are determined by multiple factors, e.g.,the individual's personal information including gender, race, education, *etc.* , as well as the contents of the image, including the color, location, size, type of objects, *etc.* .

Our study produces the first dataset of personalized saliency maps (PSMs). Specifically, we build a PSM dataset that consists of 1600 images viewed by 20 human subjects. To improve reliability, we have each image be viewed by the subject for 4 times at different time instances with a week. We use the '*Eyegaze Edge*' eye tracker to track gaze and produce a set of 32,000 $(1,600 \times 20)$ fixation maps. To correlate the acquired PSMs and the image contents, we manually segment each image into a collection of objects and semantically label them. Examples in Fig. 1 illustrate how fixations vary across three human subjects. Our annotated dataset provides fine-grained semantic analysis for studying saliency variations across individuals. For example, certain types of objects such as watches, belts introduce more variations (possibly due to gender) whereas other types such as faces produce fixation maps more coherent to the traditional universal saliency model, as shown in Table 2.

In this paper, we present a computational model towards this personalized saliency detection problem. Specially, in light of our findings that saliency maps corresponding to different persons share some commonality for the given image, which agrees with the idea of USM in existing work, we propose to model the PSM as a combination of USM and a residual map which is related to the identity and the image contents. Then we adopt a multi-task convolutional neural network (CNN) to identify the discrepancy between PSM and USM for each person, as shown in Fig. 4. Extensive experimental results demonstrate that our scheme outperforms traditional CNN approaches in accuracy.

## 2 Related Work

Tremendous efforts on saliency detection have been focused on predicting universal saliency. For the scope of our work, we only discuss the most relevant ones. We refer the readers to [Borji *et al.*, 2014] for a comprehensive study on existing universal saliency detection schemes.

**Universal Saliency Detection Benchmarks.** There are a few widely used saliency object detection and fixation prediction datasets, in which each image is generally associated with a single ground truth saliency map, averaged across the fixation maps across the participates. To select images suitable for personalized saliency, we explore several popular eye fixation datasets. The MIT dataset [Judd *et al.*, 2009] contains 1,003 images viewed by 15 subjects. In addition, the PASCAL-S [Li *et al.*, 2014] dataset provide the ground truth for both eye fixation and object detection and consist of 850 images viewed by 8 subjects. The iSUN dataset [Xu *et al.*, 2015], a large scale dataset used for eye fixation prediction, contains 20,608 images from the SUN database. The images are completely annotated and are viewed by users. Finally, the SALICON dataset [Huang *et al.*, 2015] consists of 10,000 images with rich contextual information.

**CNN Based Saliency Detection.** CNN has also been used in saliency detection. Huang *et al.* [Huang *et al.*, 2015] propose to fine-tune CNNs pre-trained for object recognition via a new objective function based on the saliency evaluation metrics such as Normalized Scanpath Saliency (NSS), Similarity, or KL-Divergence,*etc.* Pan *et al.* [Pan *et al.*, 2016] propose to use a shallow convnet trained from scratch and fine-tune a deep convnet that trained for image classification on the ILSVRC-12 dataset. Liu *et al.* [Liu *et al.*, 2015] propose a multi-resolution CNNs that are trained from image regions centered on fixation and non-fixation locations at multiscales. Srinivas *et al.* present a DeepFix [Kruthiventi *et al.*, 2015] network by using Location Biased Convolution filters to allow the network to exploit location dependent patterns. Kruthiventi *et al.* [Kruthiventi *et al.*, 2016] propose a unified framework to predict eye fixation and segment salient objects. All these approaches have focused on the universal saliency model and we show many merits of these techniques can be used for personalized saliency.

## 3 PSM Dataset

We start with constructing a dataset suitable for personalized saliency analysis.

### 3.1 Data Collection

Clearly, the rule of thumb for preparing such a dataset is to choose images that yield distinctive fixation map among different persons. To do so, we first analyze existing datasets. A majority of existing eye fixation datasets provide the one-time gaze tracking results of each individual human subject. Specifically, we can correlate the level of agreement across different observers with respect to the number of object categories in the image. When an image contains few objects, we observe that a subject tends to fix his/her gaze at locations where objects that have specific semantic meanings, eg, faces, text, signs [Judd *et al.*, 2009; Xu *et al.*, 2014]. These objects indeed attract more attention and hence are deemed more salient. However, when an image consists of multiple objects all with strong saliency as shown in Fig. 1, we observe a subject tends to diverge his/her attention. In fact, the subject focuses attention on objects that attract his/her most personally. We therefore deliberately choose 1,600 images with multiple semantic annotations to construct our dataset for PSM purpose. Among them, 1,100 images are chosen from existing saliency detection datasets including SALICON [Jiang *et al.*, 2015], ImageNet [Russakovsky *et al.*, 2015], iSUN [Xu *et al.*, 2015], OSIE[Xu *et al.*, 2014], PASCAL-S [Li *et al.*, 2014], 125 images are captured by ourselves, and 375 images are gathered from the Internet.

### 3.2 Ground truth Annotation

To gather ground truth, we have recruited 20 student participants (10 males, 10 females, aged between 20 and 24). All participants have normal or corrected-to-normal vision. In our setup, each observer sits about 40 inches in front of a 24-inches LCD monitor of a $1920 \times 1080$ resolution. All images are resized to the same resolution. We conduct all experiments in an empty and semi-dark room, with only one standby assistant. An eye tracker ('*Eyegaze Edge*' eye tracker) records their gazes as they view each image for 3 seconds. We partition 1,600 images into 34 sessions each containing 40 to 55 images. Each session lasts about 3 minutes followed by a half minute break. The eye tracker is re-calibrated at the beginning of each session. To ensure the veracity of the fixation map of each individual as well as to remove outliers, we have each image be viewed by each observer 4 times. We then combine the 4 saliency maps of the same image viewed by the same person, and use the result as the ground truth PSM of the observer. To obtain a continuous saliency map of an image from the raw data of eye tracker, we follow [Judd *et al.*, 2009] by smoothing the fixation locations via Gaussian blurs.

To find out the causes of saliency heterogeneity, we conduct the semantic segmentation for all 1,600 images via the open annotation tool LabelMe [Russell *et al.*, 2008]. Specifically, we annotate 26,140 objects of 242 classes in total, and we identify objects that attract more attention for each individual participant. To achieve this, we compare the fixation map with the mask of a specific object, and use the result as the attention value of the corresponding object. We then average the result over all images that containing the same object, and use it to measure the interestingness of the object to a specific participant. In Fig. 2, we illustrate some representative objects and persons and show the distribution of the interestingness of various objects for a same participant. We observe that all participants exhibit a similar level of interestingness measure on faces where they exhibit different interestingness measures on various objects such as watch, bow tie, *et al.* . This validates that it is necessary to choose images with multiple objects to build our PSM data.

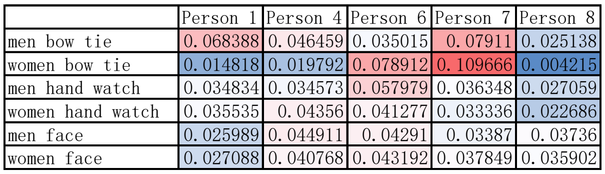

| | Person 1 | Person 4 | Person 6 | Person 7 | Person 8 |
|---|---|---|---|---|---|
| men bow tie | 0.068388 | 0.046459 | 0.035015 | 0.07911 | 0.025138 |
| women bow tie | 0.014818 | 0.019792 | 0.078912 | 0.109666 | 0.004215 |
| men hand watch | 0.034834 | 0.034573 | 0.057979 | 0.036348 | 0.027059 |
| women hand watch | 0.035535 | 0.04356 | 0.041277 | 0.033336 | 0.022686 |
| men face | 0.025989 | 0.044911 | 0.04291 | 0.03387 | 0.03736 |
| women face | 0.027088 | 0.040768 | 0.043192 | 0.037849 | 0.035902 |

Figure 2: The distribution of the interestingness of various objects for a same participant. The value is calculated as follows: we sum values of the fixation map intersecting with the mask of a specific object, and divide it with the total of fixation maps over the whole image. Thus higher value indicates that the participant puts more attention on the object.

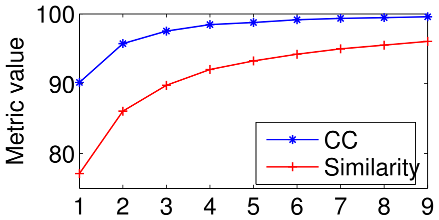

Figure 3: The point with $x = n$ measures the differences between ground truth saliency maps generated by viewing the same image n times and $n$+1 times. This figure shows that when $n$ ≥4, the ground truth saliency map generated by viewing the image n times has little difference with that generated by observing the image $n + 1$ times. Thus viewing each image 4 times is enough to get a robust estimation of the PSM ground truth.

### 3.3 Dataset Analysis

**Why view each image multiple times for ground-truth annotation?** To validate whether it is necessity to view each image multiple times, we randomly sample 220 images, and each image is viewed by the same participant 10 times. The time interval for the same person to view the same image ranges from one day to one week because we want to get the short term memory of the person for the given image. We then calculate the differences of these saliency maps in terms of the commonly used metrics for saliency detection [Judd *et al.*, 2012]: CC, Similarity. We average these criteria for all the persons and all images, and the results are shown in Fig. 3. We observe that the saliency map obtained by viewing each image only once vs. multiple times exhibit large difference. Further, the saliency map averaged over 4 or more times is closer to the long term result.

**Heterogeneity among different datasets.**To further illustrate that our proposed dataset is appropriate for personalized saliency detection task, we compare the inter-subject consistency, i.e., the agreement among different viewers, in our PSM dataset and other related datasets. Specifically, for each dataset, we first enumerate all possible subject-pairs, i.e., two different subjects, and then compute the average AUC scores across all pairs. Recall that our PSM dataset consists of images from different datasets, eg, MIT, OSIE, ImageNet, PASCAL-S, SALICON, iSUN *etc.* , and only MIT, OSIE, PASCAL-S are designed for saliency tasks[1]. Hence, we only compare the consistency scores among ours and above three datasets, and the results are shown in Table 1. We can see that our dataset achieves the lowest inter-subject consistency values among all relative ones, indicating that the heterogeneity in our saliency maps are more severe than others.

| AUC judd scores | | | |
|---|---|---|---|
| Ours | MIT | OSIE | PASCAL-S |
| **79.11** | 89.34 | 88.47 | 88.10 |

Table 1: Inter-subject consistency of different datasets. To compute the inter-subject consistency, we compute AUC judd for pair-wise saliency maps viewed by different observers for each image, then we average the results over all images. For fair comparison, the AUC judd of our method reported here is based on the saliency maps viewed by each observer once.

# 4 Approach

## 4.1 Problem Formulation

Recently, researchers [Cornia *et al.*, 2016][Pan *et al.*, 2016] have proposed to predict saliency map with CNN in an end-to-end learning strategy, and these methods have achieved state-of-the-art performance. Intuitively we could also use the same way for PSM prediction, i.e., we train a different CNN for each participant to map the RGB image to PSM directly. However, such strategy is neither scalable nor feasible for PSM because lots of training data are needed to learn a robust CNN network, thus a participant needs to observe lots of images with eye-tracker which is extremely tedious and time consuming. Furthermore, training multiple CNNs for multiple participants is also time consuming and memory expensive.

While each participant is unique in terms of their gender, race, age, personality, resulting in their heterogeneity in saliency preference, different participants still share some commonalities in their observed saliency maps because some objects, like face, logo, always attract the attention of all participants, as shown in Fig. 1. Motivated by the wisdom of universal saliency, we propose to model the PSM as a sum of Universal Saliency Map (USM) and the discrepancy between PSM and USM. In this case, only the discrepancy is identity related and image related. Mathematically, for the $n$-th participant $P_n$ ($n = 1, \ldots, N$), we define the relationship between PSM ($S_{PSM}(P_n, I_i)$), USM ($S_{USM}(I_i)$), and the discrepancy ($\Delta(P_n, I_i)$) for the given image $I_i$ ($i = 1, \ldots, K$) as follows:

$$S_{PSM}(P_n, I_i) = S_{USM}(I_i) + \Delta(P_n, I_i) \qquad (1)$$

Here the USM can be predicted by any existing saliency prediction method which discovers the commonality of a saliency map observed by different participants. Therefore, the problem of predicting PSM is converted into estimating the discrepancy $\Delta(P_n, I_i)$ , which seems to have identical difficulty as that of estimating PSM from RGB image directly. Nonetheless, as the universal saliency map $S_{USM}(I_i)$ already provides a rough estimation of the PSM, the discrepancy $\Delta(P_n, I_i)$ would work as the function of error correction, and given $S_{USM}(I_i)$, $\Delta(P_n, I_i)$ estimation is actually easier than directly estimating PSM from an RGB image [Carreira *et al.*, 2015]. Further, previous work [Carreira *et al.*, 2015] has shown that regression task would greatly benefit from such error correction strategy, and our PSM prediction actually is also a regression task. Inspired by the error correction capability of CNN [Carreira *et al.*, 2015], given $I_i$ and $S_{USM}(I_i)$, we propose a Multi-task CNN network to estimate $\Delta(P_n, I_i)$.

## 4.2 Multi-task CNN

The network architecture of our Multi-task CNN is illustrated in Fig. 4. It receives a 160 × 120 pixels RGB image along with its universal saliency map predicted by some existing saliency prediction method as its input, followed by several convolutional and pooling layers. The first four convolutional layers are shared by all participants. After the shared layers, the network is split into $N$ tasks which is exclusive for different participant. Here we suppose to have $N$ participants in total. Each task has three convolutional layers each followed by a ReLU activation function. For image $I_i$, the output of the $n$-th task corresponds to the discrepancy between PSM and USM for the $n$-th person: $\Delta(P_n, I_i)$. Previous work [Cornia *et al.*, 2016], [Lee *et al.*, 2014] has shown that by adding the supervision in middle layers, the features learned by CNN is more discriminative and boost the performance of an given task. Thus we also adapt the same idea in our Multi-task CNN, i.e., we also enforce the middle layer features of the $n$-th task to help the prediction $\Delta(P_n, I_i)$. For the $n$-th task, we use $f_\ell^n(S_{USM}(I_i), I_i) \in \mathbb{R}^{h_\ell \times w_\ell \times d_\ell} (\ell = 5, 6, 7)$ to donate the feature map after the $\ell$-th convolutional layer (the first convolutional layer corresponds to the first shared convolutional layer, so $\ell$ starts from 5). For each feature map $f_\ell^n(S_{USM}(I_i), I_i)$, we use a $1 \times 1$ convolutional layer to map it to a feature map $S_\ell(S_{USM}(I_i), I_i) \in \mathbb{R}^{h_\ell \times w_\ell \times 1}$ which corresponds to the predicted discrepancy. It is desirable that $S_\ell(S_{USM}(I_i), I_i)$ is close to $\Delta_\ell(P_n, I_i)$ which is obtained by resizing $\Delta_\ell(P_n, I_i)$ to the size of $h_\ell \times w_\ell \times 1$. Then we arrive at the following objective function:

$$\min \quad \sum_{\ell=5}^{7} \sum_{n=1}^{N} \sum_{i=1}^{K} \| S_k(S_{USM}(I_i), I_i) - \Delta_\ell(P_n, I_i) \|_F^2 \quad (2)$$

Then we use mini-batch based stochastic gradient descent to optimize all parameters in our Multi-task CNN.

[1] Even though SALICON, iSUN are also saliency fixation dataset, the ground truth of them are annotated based on records of mouse-tracking and web camera respectively.

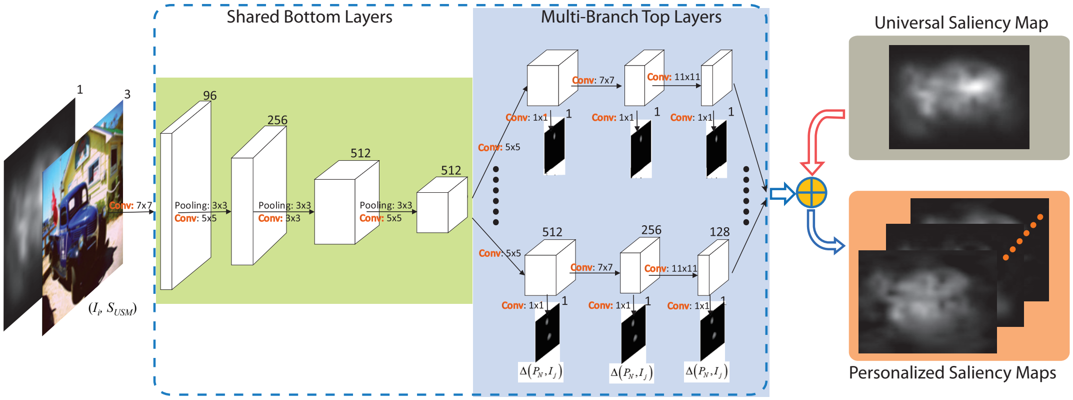

Figure 4: The pipeline of our Multi-task CNN based PSM prediction.

| Methods | CC | Similarity | AUC judd |
|---|---|---|---|
| RGB based MultiConvNets | 62.24 | 65.27 | 77.83 |
| RGB based Multi-task CNN | 64.68 | 66.28 | 79.98 |
| LDS [Fang *et al.*, 2016] | 65.73 | 63.34 | 82.96 |
| LDS + MultiConvNets | 70.71 | 75.65 | 83.69 |
| LDS + Multi-task CNN | **72.19** | **76.07** | **84.97** |
| ML-Net [Cornia *et al.*, 2016] | 41.35 | 51.30 | 71.80 |
| ML-Net + MultiConvNets | 65.35 | 79.42 | 81.70 |
| ML-Net + Multi-task CNN | **67.53** | **80.17** | **83.45** |
| BMS [Zhang and Sclaroff, 2013] | 59.59 | 71.36 | 80.26 |
| BMS + MultiConvNets | 68.68 | 79.66 | 83.79 |
| BMS + Multi-task CNN | **70.33** | **80.41** | **85.03** |
| SalNet [Pan *et al.*, 2016] | 72.66 | 74.18 | 84.67 |
| SalNet + MultiConvNets | 74.85 | 77.89 | 85.09 |
| SalNet + Multi-task CNN | **76.28** | **79.08** | **85.94** |

Table 2: The performance comparison of difference methods on our PSM dataset.

**Remarks:** Compared with using separate CNNs to predict $\Delta(P_n, I_i)$ for different participants, our Multi-task CNN architecture has the following advantages: i)previous work [Li *et al.*, 2016], [Zhang *et al.*, 2014] has shown that features extracted by the first several layers can be shared between multiple tasks (Each task in our paper corresponding to the predication of the discrepancy for each observer), thus our shared layers architecture reduces the number of parameters and the memory cost. Furthermore, all training samples from all participants can be fully utilized to train the parameters corresponding to these shared layers, which simplifies the network training procedure and boosts the accuracy; ii) Since the first few layers are shared and trained by all participants in the training set, it can be easily adapted to some participants who are not in our dataset, and makes the PSM prediction for these unseen subjects easier. Thus such multi-task framework makes the problem scalable for open set setting.

# 5 Experiments

## 5.1 Experimental Setup

**Parameters.** Our method is implemented based on the CAFFE framework developed by Jia *et. al.* [Jia *et al.*, 2014]. We train our network with the following hyper-parameters setting: mini-batch size (40), learning rate (0.0003), momentum (0.9), weight decay (0.0005), number of iterations (40,000). The network architecture of our Multi-task CNN is identical to that of DeepNet [Pan *et al.*, 2016] except for that i) the parameters corresponding to taskes of different participants are different; ii) middle layer supervision is imposed by adding 1 *conv* layer after *conv5* and *conv6*; iii) an channel corresponding to USM is added in the input. We use the provided DeepNet model to initialize the corresponding parameters in our model, thus all networks are initialized with the same parameters. The parameters corresponding to the universal saliency map channel and 1 *conv* layers for middle layer supervision are initialized with 'xavier'. Such using well-trained network model for parameter initialization strategy has been demonstrated their effectiveness for performance improvement in both saliency detection [Pan *et al.*, 2016] and image segmentation task[Kruthiventi *et al.*, 2016]. In our experiments, 600 images are randomly selected as training data, and the remaining 1,000 images are used for testing data. We augment the training data through left-right flip operations to avoid over-fitting and improve the robustness of our model.

**Baselines.** All existing fixation prediction methods can be used to generate an universal saliency map. Based on the performance of existing methods on the MIT saliency benchmark [Bylinskii *et al.*, ] in terms of similarity, we choose LDS [Fang *et al.*, 2016], BMS [Zhang and Sclaroff, 2013], ML-Net [Cornia *et al.*, 2016], and SalNet [Pan *et al.*, 2016] to predict the universal saliency maps on our dataset. Of these four methods, the first two methods are based on hand-crafted features, and the latter two are based deep learning methods. The source codes and the saliency prediction models provided by these four methods are used in our experiments. Then we use the RGB image and predicted USM to predict PSM for each participant. We compare our method with the following three baselines: i) We also use USM to help to predict the discrepancy between the PSM and USM, but different ConvNets are trained for different participants. Since multiple ConvNets are trained for these baselines, we term such baselines as LDS+MultiConvNets, and BMS+MultiConvNets, MLNet+MultiConvNets,and SalNet+MultiConvNets, respectively. DeepNet architecture is used for these baselines; ii) We use RGB image as the input to train a CNN for PSM prediction directly. Different CNNs are trained for different participants. This baseline is termed as RGB based MultiConvNets. DeepNet architecture is also used for this baseline; iii) We use RGB image as the input to train a CNN for PSM prediction directly. Different from RGB based MultiConvNets, we use the Multi-task CNN architecture. This baseline is termed as RGB based Multi-task CNN. For this baseline method, the CNN is exactly the same with our method. We can see that the network architectures of all baselines are similar to that of our method except that i) input and the number input channels, ii) whether the parameters are shared in the first few layers. For all baseline methods, we use the same way for parameter initialization, i.e., use the DeepNet model to initialize the parameters. The supervision on middle layers is also used for all baselines. The same data augmentation strategy is used for all baselines. Therefore, the comparisons between our method and these baselines are fair.

**Measurements.** Following the most existing works [Liu *et al.*, 2015], [Pan *et al.*, 2016], [Kruthiventi *et al.*, 2016], we use CC, Similarity, and AUC judd [Judd *et al.*, 2012] as metrics to evaluate the differences between the predicted saliency map and ground truth.

## 5.2 Performance Evaluation

The performance of all methods are listed in Table 2. We can see that our solution always achieves the best performance in terms of all metrics, which demonstrates the effectiveness of our method. Further, we can see that i) USM based personalized saliency detection methods always outperform that of directly predicting PSM from RGB images, which validates the effectiveness of "error correction" strategy for personalized saliency detection. In other words, USM boosts the result of personalized saliency prediction; Further, the poor performance of PSM prediction directly from RGB images may result from the lack of enough training samples. By leveraging the USM and Multi-task CNN, our method greatly outperforms PSM prediction directly from RGB images, which further proves the effectiveness of our method. ii) Multi-task CNN based methods always outperform MultiConvNets methods.

**The effect of supervision on middle layers** Fig.5 shows the accuracy gain of imposing supervision on middle layers in our Multi-task CNN. We can see that middle layer supervision helps the PSM prediction, which agrees with existing findings [Lee *et al.*, 2014].

**The effect of the number of training samples on the PSM prediction accuracy.** Fig.6 shows that when we increase the number of training samples from 200 to 600 (the testing data are fixed.) the testing accuracy can be improved. As we known, training a more robust deep network requires large-scale training samples. However, with the limitation in data collecting equipments, data acquisition procedure is very time consuming, thus it is very cost expensive to get enough training samples for network training.

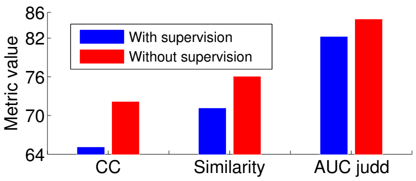

Figure 5: The effect of supervision on middle layers in our Multi-task CNN.

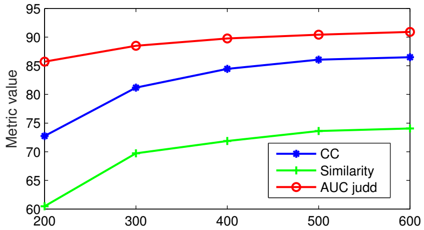

Figure 6: The effect of the number of training samples on the accuracy of PSM prediction.

# 6 Conclusion and Future Work

Recent psychology studies suggest that saliency is highly specific than universal. Motivated by the potential applications of PSM, in this paper, we first study the task of personalized saliency detection. Especially, we build the first PSM dataset and propose to model the PSM as a combination of USM and the discrepancy between PSM and USM. Then we propose a Multi-task CNN framework for the prediction of this discrepancy. Comprehensive experiments demonstrate that our PSM prediction scheme is effective and reliable.

This is a preliminary study about personalized saliency, and our method is the first attempt along this direction, and there is huge space to improve our work. Since it is extremely tedious and time consuming for a participant to observe lots of images, our dataset is limited, in terms of the number of images and participants. Further, we also find that such personalized saliency is closely related to the observers' personal information, including gender, race, major, *etc.* , and these information is easy to collect. Therefore, we believe by incorporating these personal information in PSM prediction, the performance of PSM prediction can be further boosted, meanwhile the number of training samples would be greatly reduced, which would make PSM prediction more scalable in real applications.

## References

[Borji *et al.*, 2014] Ali Borji, Ming Ming Cheng, Huaizu Jiang, and Jia Li. Salient object detection: A survey. *Eprint Arxiv*, 16(7):3118, 2014.

[Bylinskii *et al.*, ] Zoya Bylinskii, Tilke Judd, Ali Borji, Laurent Itti, Frédo Durand, Aude Oliva, and Antonio Torralba. Mit saliency benchmark.

[Carreira *et al.*, 2015] Joao Carreira, Pulkit Agrawal, Katerina Fragkiadaki, and Jitendra Malik. Human pose estimation with iterative error feedback. *arXiv preprint arXiv:1507.06550*, 2015.

[Chang *et al.*, 2016] Miko May Lee Chang, Soh Khim Ong, and Andrew Yeh Ching Nee. Automatic information positioning scheme in ar-assisted maintenance based on visual saliency. In *SAIENTO AVR*, pages 453–462. Springer, 2016.

[Cornia *et al.*, 2016] Marcella Cornia, Lorenzo Baraldi, Giuseppe Serra, and Rita Cucchiara. A deep multilevel network for saliency prediction. *arXiv preprint arXiv:1609.01064*, 2016.

[Fang *et al.*, 2016] S. Fang, J. Li, Y. Tian, T. Huang, and X. Chen. Learning discriminative subspaces on random contrasts for image saliency analysis. *TNNLS*, 2016.

[Gygli *et al.*, 2013] Michael Gygli, Helmut Grabner, Hayko Riemenschneider, Fabian Nater, and Luc Van Gool. The interestingness of images. In *ICCV*, pages 1633–1640, 2013.

[Huang *et al.*, 2015] Xun Huang, Chengyao Shen, Xavier Boix, and Qi Zhao. Salicon: Reducing the semantic gap in saliency prediction by adapting deep neural networks. In *ICCV*, pages 262–270, 2015.

[Itti, 2004] Laurent Itti. Automatic foveation for video compression using a neurobiological model of visual attention. *IEEE TIP*, 13(10):1304–1318, 2004.

[Jia *et al.*, 2014] Yangqing Jia, Evan Shelhamer, Jeff Donahue, Sergey Karayev, Jonathan Long, Ross Girshick, Sergio Guadarrama, and Trevor Darrell. Caffe: Convolutional architecture for fast feature embedding. *arXiv preprint arXiv:1408.5093*, 2014.

[Jiang *et al.*, 2015] Ming Jiang, Shengsheng Huang, Juanyong Duan, and Qi Zhao. Salicon: Saliency in context. In *CVPR*, pages 1072–1080, 2015.

[Judd *et al.*, 2009] Tilke Judd, Krista Ehinger, Frédo Durand, and Antonio Torralba. Learning to predict where humans look. In *ICCV*, pages 2106–2113, 2009.

[Judd *et al.*, 2012] Tilke Judd, Frédo Durand, and Antonio Torralba. A benchmark of computational models of saliency to predict human fixations. In *MIT Technical Report*, 2012.

[Kruthiventi *et al.*, 2015] Srinivas SS Kruthiventi, Kumar Ayush, and R Venkatesh Babu. Deepfix: A fully convolutional neural network for predicting human eye fixations. *arXiv preprint arXiv:1510.02927*, 2015.

[Kruthiventi *et al.*, 2016] Srinivas S. S. Kruthiventi, Vennela Gudisa, Jaley H. Dholakiya, and R. Venkatesh Babu. Saliency unified: A deep architecture for simultaneous eye fixation prediction and salient object segmentation. In *CVPR*, pages 5781–5790, 2016.

[Lee *et al.*, 2014] Chen Yu Lee, Saining Xie, Patrick Gallagher, Zhengyou Zhang, and Zhuowen Tu. Deeply-supervised nets. *Arxiv*, pages 562–570, 2014.

[Li *et al.*, 2014] Yin Li, Xiaodi Hou, Christof Koch, James M Rehg, and Alan L Yuille. The secrets of salient object segmentation. In *CVPR*, pages 280–287, 2014.

[Li *et al.*, 2016] X. Li, L. Zhao, L. Wei, M. H. Yang, F. Wu, Y. Zhuang, H. Ling, and J. Wang. Deepsaliency: Multi-task deep neural network model for salient object detection. *TIP*, 25(8):3919–3930, 2016.

[Liu *et al.*, 2015] Nian Liu, Junwei Han, Dingwen Zhang, Shifeng Wen, and Tianming Liu. Predicting eye fixations using convolutional neural networks. In *CVPR*, pages 362–370, 2015.

[Pan *et al.*, 2016] Junting Pan, Elisa Sayrol, Xavier Giroinieto, Kevin Mcguinness, and Noel E. Oconnor. Shallow and deep convolutional networks for saliency prediction. In *CVPR*, pages 598–606, 2016.

[Russakovsky *et al.*, 2015] Olga Russakovsky, Jia Deng, Hao Su, Jonathan Krause, Sanjeev Satheesh, Sean Ma, Zhiheng Huang, Andrej Karpathy, Aditya Khosla, Michael Bernstein, Alexander C. Berg, and Li Fei-Fei. ImageNet Large Scale Visual Recognition Challenge. *IJCV*, 115(3):211–252, 2015.

[Russell *et al.*, 2008] Bryan C Russell, Antonio Torralba, Kevin P Murphy, and William T Freeman. Labelme: a database and web-based tool for image annotation. *IJCV*, 77(1-3):157–173, 2008.

[Setlur *et al.*, 2005] Vidya Setlur, Saeko Takagi, Ramesh Raskar, Michael Gleicher, and Bruce Gooch. Automatic image retargeting. In *MUM*, pages 59–68, 2005.

[Xu *et al.*, 2014] Juan Xu, Ming Jiang, Shuo Wang, Mohan S Kankanhalli, and Qi Zhao. Predicting human gaze beyond pixels. *Journal of vision*, 14(1):28–28, 2014.

[Xu *et al.*, 2015] Pingmei Xu, Krista A Ehinger, Yinda Zhang, Adam Finkelstein, Sanjeev R Kulkarni, and Jianxiong Xiao. Turkergaze: crowdsourcing saliency with webcam based eye tracking. *arXiv preprint arXiv:1504.06755*, 2015.

[Zhang and Sclaroff, 2013] Jianming Zhang and Stan Sclaroff. Saliency detection: A boolean map approach. In *ICCV*, pages 153–160, 2013.

[Zhang *et al.*, 2014] Zhanpeng Zhang, Ping Luo, Change Loy Chen, and Xiaoou Tang. Facial landmark detection by deep multi-task learning. In *ECCV*, pages 94–108, 2014.